Second-order cues to figure motion enable object detection during prey capture by praying mantises

Vivek Nityananda[a,1], James O'Keeffe[a], Diana Umeton[a], Adam Simmons[a], and Jenny C. A. Read[a]

[a]Biosciences Institute, Faculty of Medical Sciences, Newcastle University, NE2 4HH Newcastle upon Tyne, United Kingdom

Edited by Raghavendra Gadagkar, Indian Institute of Science, Bangalore, India, and approved November 7, 2019 (received for review July 18, 2019)

Detecting motion is essential for animals to perform a wide variety of functions. In order to do so, animals could exploit motion cues, including both first-order cues—such as luminance correlation over time—and second-order cues, by correlating higher-order visual statistics. Since first-order motion cues are typically sufficient for motion detection, it is unclear why sensitivity to second-order motion has evolved in animals, including insects. Here, we investigate the role of second-order motion in prey capture by praying mantises. We show that prey detection uses second-order motion cues to detect figure motion. We further present a model of prey detection based on second-order motion sensitivity, resulting from a layer of position detectors feeding into a second layer of elementary-motion detectors. Mantis stereopsis, in contrast, does not require figure motion and is explained by a simpler model that uses only the first layer in both eyes. Second-order motion cues thus enable prey motion to be detected, even when perfectly matching the average background luminance and independent of the elementary motion of any parts of the prey. Subsequent to prey detection, processes such as stereopsis could work to determine the distance to the prey. We thus demonstrate how second-order motion mechanisms enable ecologically relevant behavior such as detecting camouflaged targets for other visual functions including stereopsis and target tracking.

second-order motion | stereo vision | motion detection | model | camouflage

Animals must detect motion for several vital functions, including navigation and postural stability. One important function is prey capture, since prey are often given away by their motion. Whereas navigation and postural stability can exploit motion across the entire visual field, prey capture usually involves detecting the motion of specific targets. This motion can be either *figure motion*, where an object moves across the visual field (1–3) (e.g., a bird flying across the sky), or *elementary motion* within a restricted region of the visual field (e.g., a bird flapping its wings while stationary).

Motion could potentially be detected by several means, including the detection of both first- and second-order motion. First-order motion involves correlations in luminance at different positions over time, such as might be seen when a dark bug moves against a bright background. Second-order motion detection, however, involves correlations of higher-order visual statistics. Humans can detect second-order motion, for example, when contrast changes move across a static pattern (4–6). Sensitivity to second-order motion has also been unequivocally reported from 1 insect—the fruit fly—and this was the first demonstration of this capability in invertebrates (1, 7–9). This sensitivity allows flies to track figure motion, even when elementary motion moves in the opposite direction or is absent.

Natural moving stimuli can have complex visual statistics, but typically contain correlations of luminance changes across space and time (i.e., Fourier motion), which can be detected by first-order motion detectors like the Hassenstein–Reichardt detector (10–12). It is therefore unclear why further mechanisms to detect second-order motion have evolved. One possibility is simply that this makes motion detection more robust. Many types of second-order motion detectors will detect the first-order motion (refs. 13–15 and our model below) of moving targets. Second-order motion cues can also increase sensitivity to signals when combined with first-order cues (16). This could be particularly important if animals have evolved to reduce first-order motion cues as a form of camouflage. For example, an animal which managed to be entirely featureless and equal in luminance to the average for the environment in which it moved would produce little first-order motion (17) and none at all when evaluated over scales that are large compared to the background texture. Such an animal would, however, have cues to second-order motion consisting of changes in contrast as it occluded different regions of the background. Thus, by evolving second-order motion detectors, an animal may improve its ability to detect all forms of motion, especially those selected to be cryptic.

Object detection is also important in stereo vision. Stereo vision exploits the disparity between the views of the 2 eyes to compute depth. This ability has been well studied in vertebrates (18–21), especially primates (22–25), though less is known about the mechanisms of stereopsis in invertebrates (26–33). Importantly, it has been suggested that vertebrate stereopsis has evolved to break camouflage and better enable object perception by highlighting object contours that differ in depth to the background (26, 34). In primates, this is achieved by cross-correlating the patterns of luminance between the 2 eyes. Recent work has shown that mantis stereo vision differs from primate and avian stereo vision in this regard (30). Mantis strikes to moving stimuli remain sensitive to stereoscopic depth, even in the absence of any luminance correlation between the eyes, instead exploiting the position of image

Significance

Insects are sensitive to second-order motion and can detect changing patterns without correlating first-order visual statistics. The adaptive value of this sensitivity to second-order motion and the role it plays in natural behavior is still unclear. Here, we show that it is fundamental to prey detection in praying mantises, which is combined with a separate mechanism for stereopsis to enable accurate distance-dependent prey capture. We present a model of mantis second-order motion detection that explains our behavioral results and is consistent with the current knowledge of insect motion detection. Our results demonstrate an ecological function that second-order motion sensitivity could perform during object and prey detection by animals.

Author contributions: V.N. and J.C.A.R. designed research; V.N., D.U., and A.S. performed research; V.N. analyzed data; J.O.K. and J.C.A.R. implemented the computational model; and V.N., J.O.K., and J.C.A.R. wrote the paper.

The authors declare no competing interest.

This article is a PNAS Direct Submission.

Data deposition: Data are available on Figshare at https://doi.org/10.6084/m9.figshare.8944910.v1.

[1]To whom correspondence may be addressed. Email: vivek.nityananda@ncl.ac.uk.

This article contains supporting information online at https://www.pnas.org/lookup/suppl/doi:10.1073/pnas.1912310116/-/DCSupplemental.

motion in the 2 eyes. Mantis stereopsis thus even outperforms human stereo for moving stimuli with poor interocular luminance correlation. Furthermore, this mechanism enables mantises to discriminate stereoscopic depth, even in stimuli with no coherent first-order motion (30). An extensive literature on mantis predation also suggests that figure motion with particular characteristics (speed and location in the visual field) is necessary for eliciting predatory behavior (27, 29, 30, 32). Yet, all work on mantis stereopsis to date has used stimuli with figure motion, and it has not been tested with stimuli presenting elementary motion alone. Thus, it remains unclear whether mantis stereopsis responds to elementary motion.

Taken together, this suggests the hypothesis that praying mantises could capture prey based on the detection of figure motion via second-order motion mechanisms. In this paper, we set out to test this hypothesis. We investigated the contributions of figure and elementary motion, with and without first-order motion cues, to mantis prey detection, and additionally to mantis stereopsis.

Results

Behavioral Experiments. In experiment 1, we tested the ability of mantises to detect prey and perceive stereoscopic depth in stimuli with different combinations of first- and second-order motion cues. Mantises viewed the stimuli in a stereoscopic (3D) insect cinema while wearing color filters with different colors for each eye, enabling us to present them anaglyph 3D stimuli (29, 32). The screen was placed 10 cm away from the mantis, which is too far for 2D visual stimuli to elicit a strike for prey capture but can still elicit visual tracking (35). In our experiments, we defined a predatory response as either a strike (a rapid extension of the forelegs) or a tension (a preparatory movement for a strike which is not followed by one) (29, 36). All experiments had interleaved stimuli with 2 disparity conditions: crossed and uncrossed. In the crossed-disparity condition (Fig. 1*A*), the parallax was chosen to simulate a target 2.5 cm in front of the mantis—a distance at which stimuli elicit prey-capture responses. In the uncrossed-disparity condition, stimuli had the same parallax but with the left and right positions swapped. Since the lines of sight did not cross in the latter condition, and the parallax was larger than the mantis interocular distance, this meant that the distance of the visual target from the mantis was undefined and would not elicit strikes (29). This acts as a control to test whether responses to the crossed condition are driven by the stereoscopically defined distance. We presented the mantises with stimuli having differing first- and second-order motion content in both of these disparity conditions. We used 4 types of motion stimuli previously used to investigate insect sensitivity to second-order motion: Fourier, theta, drift-balanced, and small-field motion (3, 7–9, 13, 37) (Fig. 1 *B–E*), described in turn below. For Fourier amplitude spectra for these stimuli, see Fig. 5 *B–E*. Note that these 4 stimuli differ only in their temporal structure and are indistinguishable on the basis of a single frame.

First, we asked how mantises respond to Fourier motion stimuli. These are the most natural moving stimuli, which are detected by first-order motion detectors and some models of second-order motion detectors (13, 14). The direction of motion detected by both types of detectors is the same for these stimuli. We know that mantises discriminate depth and initiate prey capture in response to suitable Fourier motion stimuli, e.g., a black disk spiraling over a brighter background (29). Here, we used horizontal Fourier motion of a target as a baseline to compare with other types of motion. The target was a circular patch of dots that moved from one side of the screen to the other over a background composed of similar dots (Fig. 1*B* and Movie S1). The dots were large enough to be individually resolvable, given the low spatial acuity of the mantis's eyes and the elementary motion of the dots matched the figure motion of the disk. This is similar to a spotted bug moving against the background, where both the bug and the spots on its back have the same motion. Mantises could detect these stimuli and were significantly more likely to respond to crossed rather than uncrossed disparities (generalized linear mixed model [GLMM]: effect size estimate = 2.96, $P = 7.64 \times 10^{-5}$; Fig. 1*B*); data for all results available at ref. 38.

We next investigated mantis responses to stimuli with theta motion (14), where elementary motion and figure motion are in opposite directions. For these stimuli, first- and second-order motion detectors detect opposite directions of motion, with first-order mechanisms tracking the direction of elementary motion and second-order mechanisms tracking the direction of figure motion (13, 14). The stimulus here was the same as the stimulus described above, but here the dots within the target streamed in the opposite direction to the motion of the targets they comprised (Fig. 1*C* and Movie S2). Since the different motion cues are in conflict here, if prey detection or stereopsis were sensitive to the direction of motion, the mantises could potentially make more errors when presented with these stimuli. Mantises were, however, responsive to theta motion stimuli and were again significantly more likely to respond to crossed compared to uncrossed disparities (GLMM: effect size estimate = 1.90, $P = 2.37 \times 10^{-6}$; Fig. 1*C*). Thus, mantis prey capture and stereopsis can discriminate depth, even when first-order and second-order motion detectors detect opposite directions. Interestingly, response probabilities to the theta condition were significantly greater than for all other conditions, indicating that a particular combination of figure and elementary motion generates the greatest response (GLMM: theta vs. Fourier: effect size = 0.98, $P = 5.03 \times 10^{-4}$; theta vs. drift-balanced: effect size = 0.5993, $P = 0.0252$; theta vs. small-field: effect size = 4.78, $P = 2.99 \times 10^{-6}$).

We were next interested in the relative contribution of first- and second-order motion mechanisms to prey capture responses. To investigate this, we used stimuli that eliminated elementary and figure motion in turn. We first asked whether first-order elementary motion was necessary at all for prey detection and stereoscopic depth discrimination. To do so, we presented mantises with "drift-balanced" stimuli (37) where the dots have no motion but the figure moves—creating the effect of a circular window moving on the background, revealing a different background beneath (Fig. 1*D* and Movie S3). Since the dot patterns on either side of the edge of the circular window are different but have the same average luminance, the average correlation across time and space is 0. First-order motion detectors might be activated by random fluctuations in correlation, but, on average, the activity would be the same in first-order motion detectors tuned to opposite directions. These stimuli, therefore, have no net first-order motion, and this experiment thus tested the idea that mantises require first-order motion to detect targets. Mantises detected these stimuli and responded significantly more to crossed compared to uncrossed disparities (GLMM: effect size estimate = 2.02, $P = 1.93 \times 10^{-5}$; Fig. 1*D*), showing that first-order elementary motion is not necessary for either prey detection or stereopsis.

Finally, we presented the mantises with a stimulus which had elementary small-field motion, but no figure motion (Fig. 1*E* and Movie S4), testing the idea that elementary first-order motion would be sufficient to elicit mantis prey-capture responses. Here, dots streamed within a circular window, with dots continually entering from one side of the window and vanishing when they reached the other side, but the window itself stayed fixed. Previous research into the mechanisms of mantis stereopsis suggested that it was tuned to simultaneous temporal change in specific positions in each eye (30). This would imply that stereopsis would enable mantises to discriminate depth when this temporal change corresponded to just elementary motion without any figure motion cues, as was the case here. However,

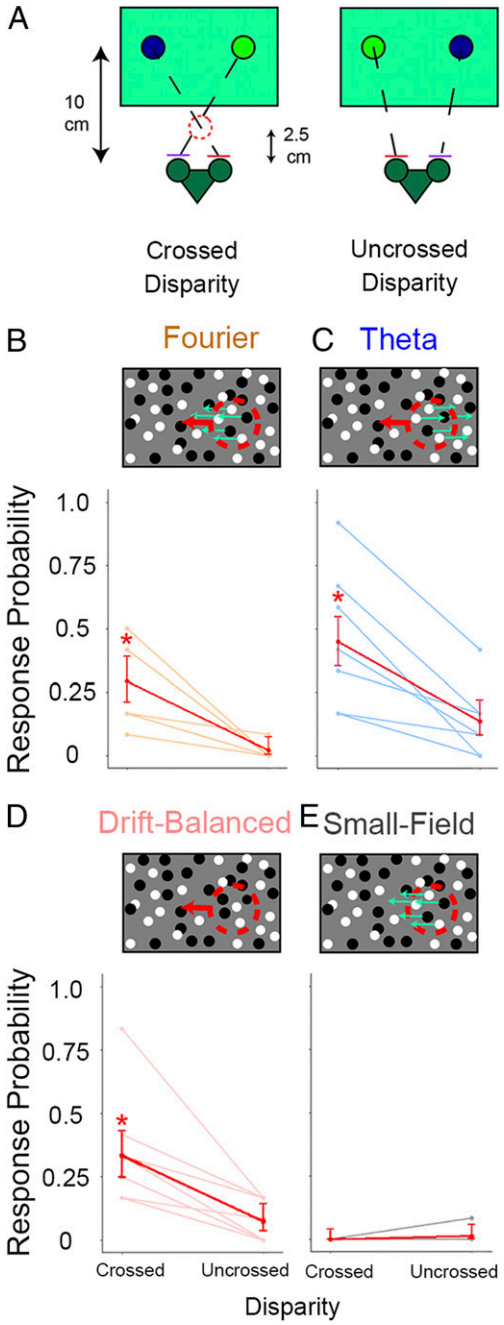

Fig. 1. Experiment 1: Stimuli and prey-capture responses. (*A*) Color filters were attached to the mantis to enable the presentation of 3D anaglyph stimuli. Mantises viewed the stimuli from a distance of 10 cm and were free to strike at stimuli with their forearms. All stimuli were presented in both crossed- and uncrossed-disparity conditions. Crossed-disparity conditions simulated a target (dotted red circle) 2.5 cm from the mantis, in their catch range. Uncrossed-disparity conditions had the same parallax as the crossed-disparity stimuli, but with left and right swapped. Since this parallax was greater than the interocular distance of the mantises, the distance to the mantis was undefined. (*B*–*E*) Cartoons of stimuli above responses (strikes and tensions) to the stimuli in experiment 1. (*B*) Fourier stimuli (Movie S1): First-order elementary motion (thin green arrows) had the same speed and direction as the figure motion (thick red arrow). (*C*) Theta stimuli (Movie S2): First-order elementary motion (green arrows) had the same speed but the opposite direction to the second-order figure motion (red arrow). (*D*) Drift-balanced stimuli: A circular moving window revealed a different pattern of dots apparently seen through the window (Movie S3). Thus, there were no moving dots, and only second-order figure motion (red arrow) was present without any first-order elementary motion. (*E*) Small-field motion: Only first-order elementary motion (green arrow) was present without any figure motion (Movie S4). Bold red lines in the responses represent the probability of prey-capture responses (strikes + tensions) across all animals. Lighter lines represent data from individuals. $*P < 0.05$. Error bars represent 95% binomial confidence intervals.

mantises barely responded to these stimuli, and it was impossible to statistically compare their responses to crossed and uncrossed disparities (Fig. 1*E*). This suggests that prey detection and capture by mantises depends on the cues to figure motion. First-order elementary motion, when presented alone, was thus insufficient for eliciting stereopsis-dependent predatory responses in the mantis.

To verify these results and further assess the role of first-order motion, we first replicated the results of the drift-balanced and Fourier motion experiments in experiment 2, using a spiral stimulus that has been shown to be attractive to mantises (29, 30). Because the direction of motion was constantly changing in this spiral stimulus, we did not attempt to create a version of this stimulus with theta motion. We presented the mantises with 3 stimuli. The first consisted of a drift-balanced stimulus as described above, but with the spiraling motion (Fig. 2*A*). The second stimulus was a "luminance flipped stimulus" (30), consisting of a spiraling target region within which the background dots changed their luminance from black to white and vice versa as the region passed over them (Fig. 2*B*; also depicted with left–right motion in Movie S5). Note that this stimulus differed from the drift-balanced stimulus in that the dots that changed their luminance were already present in the background, but changed as the target area moved over them. In the case of the drift-balanced stimulus, the dots within the target were a different pattern compared to the background. The third stimulus was a Fourier disk stimulus, where a disk of dots moved in a spiraling motion obscuring the background dots behind it (Fig. 2*C*). All 3 stimuli were presented in both crossed and uncrossed disparities. The first 2 stimuli tested mantis depth discrimination in second-order motion without any coherent first-order motion cues, and the third stimulus was a positive control with clear first- and second-order motion cues in the same direction.

Strike probability across all 3 stimuli showed a significant main effect of disparity (GLMM: effect size estimate = 3.64, $P < 2 \times 10^{-16}$; Fig. 2), implying that the mantises were able to discriminate depth in all 3 conditions. Since this was true even for the drift-balanced and luminance flipped stimuli that lacked first-order motion, these results confirm that first-order motion is not necessary for prey detection and stereoscopic depth perception in mantises.

Our results show that figure motion elicits strikes whether containing first-order motion or not, but that elementary first-order motion, without figure motion of the target, does not elicit strikes for either disparity. This suggests that either prey detection or stereopsis requires figure motion of a target across the visual field and is insensitive to localized elementary motion without the motion of a figure. One possibility is that mantis stereoscopic vision is intrinsically sensitive to disparity defined by elementary motion, but that figure motion is required to activate a separate prey-detection system and release the strike.

To test this possibility, in experiment 3, we designed a stimulus where a stationary target, with only internal elementary motion and no second-order figure motion, was preceded by a spiraling target consisting of a drift-balanced stimulus with no elementary motion (Fig. 3). Experiment 2 demonstrated that the drift-balanced spiral was attractive to mantises and that they can discriminate depth in this stimulus. In separate trials, the spiraling target was presented with crossed disparity at a virtual distance of

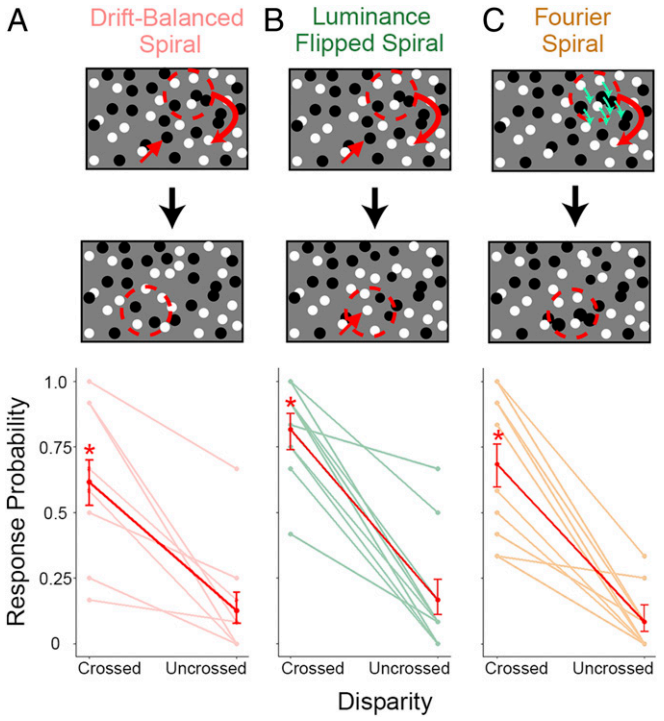

Fig. 2. Experiment 2: Stimuli and prey capture responses. Strikes and tensions in response to drift-balanced spiral stimuli (*A*), luminance-flipped spiral stimuli (*B*), and Fourier disk spiral stimuli (*C*). Other details are as in Fig. 1. Stimulus cartoons depicted above the results depicted early and later frames of the stimulus. (*A*) Background dots in the drift-balanced condition were replaced by a new pattern as the window passed over them (e.g., dot indicated by red arrow in the top frame has no counterpart in the bottom frame, since this region is now within the target and has thus been replaced by a new random dot pattern). Dots within the target region were stationary but differed as the target moved (compare pattern within the dashed ring in one frame with the corresponding region in the other frame: The dot patterns are unrelated). (*B*) Background dots in the luminance-flipped spiral remained in the same position, but changed luminance from black to white and vice versa when the target region moved over them (pattern within the dashed ring in one frame is the same as for the corresponding region in the other frame, but with contrast polarity inverted; e.g., dot indicated by red arrows in the top and bottom frames). (*C*) In the Fourier condition, a coherent dot patch moved over the background dots and obscured them (pattern within the dashed ring is the same in the top and bottom frames, just displaced in the image). $*P < 0.05$.

either 5 or 2.5 cm until it reached the center, where it vanished. A second later, the final elementary motion-only target was shown with either a crossed or uncrossed disparity. The magnitude of the disparity was the same in these 2 elementary motion conditions and conveyed a target distance of 2.5 cm in the crossed condition. The idea was that the spiraling figure motion would activate the prey-detection system and prime the mantis to release the strike when the final target appeared at the center. If mantis stereopsis can discriminate disparity in purely elementary motion, then we would expect more strikes to be released when the target reappeared in the catch range (crossed disparity) than at an undefined distance (uncrossed disparity). This experiment thus tested whether mantises would use purely first-order elementary motion to discriminate a target's depth if their prey-detection system had been activated previously with a target defined purely by second-order figure motion. We classified any strikes according to whether they occurred during the spiral figure-motion phase or during the later elementary-motion phase and only analyzed the strikes that occurred during the second phase. If mantises could discriminate depth in the second phase after identifying a target in the first phase, we would expect to see a difference between responses to crossed and uncrossed disparities in this phase. In addition, if mantis responses in the second phase were influenced by the distance of the target in the first phase, we would expect differential responses in the second phase when motion in the first phase was simulated to be at 2.5 cm compared to 5 cm.

In the second, elementary-motion, phase we found that mantises were significantly more likely to respond to and strike at the target in the crossed-disparity condition compared to the uncrossed-disparity condition (responses: GLMM: effect size estimate: 3.51, $P < 2 \times 10^{-16}$ [Fig. 3, *Upper*]; strikes: GLMM: effect size estimate: 4.17, $P = 5.08 \times 10^{-16}$ [Fig. 3, *Lower*]). This indicates that mantis stereopsis is also sensitive to the disparity of a stationary target defined by elementary motion. The depth of the preceding figure motion also had a significant effect on the probability of striking (GLMM: effect size estimate: −1.04, $P = 3.76 \times 10^{-4}$). Moving prey perceived to be closer in the first phase was more likely to elicit strikes, but mantises discriminated disparity, even if the moving prey was initially perceived to be further away. Thus,

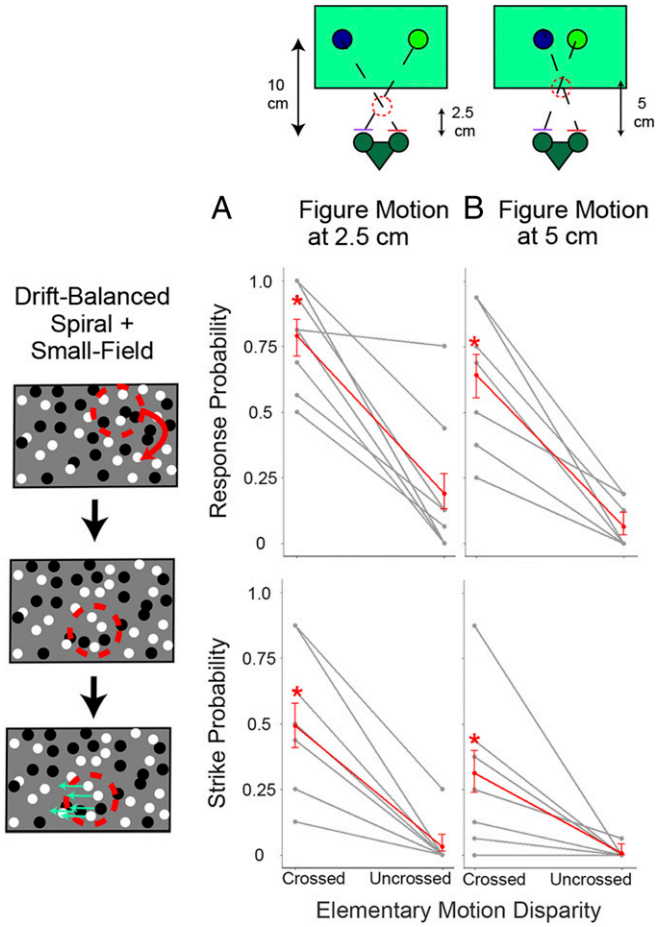

Fig. 3. Experiment 3: prey-capture responses. The responses are to the elementary-motion phase of the stimulus. The preceding figure motion simulated distances of 2.5 cm (*A*) and 5 cm (*B*). Bold red lines represent the probability of prey-capture responses (strikes + tensions; *Upper*) or strikes (*Lower*) across all animals. Other details are as in Fig. 1. Stimulus cartoon in *Left* depicts the initial drift-balanced spiral (Fig. 2*A*) with figure motion and the later small-field motion (Fig. 1*E*) with elementary motion. Stimulus cartoon at *Top* depicts the 2 disparity conditions of the figure motion with simulated target depths of 2.5 and 5 cm. $*P < 0.05$.

once moving prey is detected at either distance, the stereo system can distinguish disparity using either figure motion (experiments 1 and 2) or elementary motion (experiment 3).

Experiment 3 shows that mantis stereopsis can discriminate disparity in stimuli with only elementary motion, when primed by figure motion at disparities within a mantis's catch range. In a final experiment—experiment 4—we asked whether the preceding figure motion had to have a disparity in the mantis's catch range in order to have this priming effect. To test this, we ran a version of the experiment where the spiral stimulus that preceded the target had uncrossed disparity. The "priming" stimulus thus provided binocular stimulation, but its geometry did not convey a coherent distance to a target. If mantis stereopsis requires priming by figure motion with crossed disparity, we would not see disparity-selective strikes to elementary-motion targets following figure motion with uncrossed disparity. In this experiment, rather than the figure motion indicating a spiral at 2.5 or 5 cm (as in experiment 3), it indicated either a crossed target at 2.5 cm or an uncrossed one with the same magnitude of parallax. Each of these conditions was then followed by the crossed or uncrossed elementary motion. We found that in the second, elementary-motion phase, mantises still discriminated between crossed and uncrossed disparities for both responses overall (GLMM: estimate = 3.71, $P < 2 \times 10^{-16}$; Fig. 4, *Upper*) and strikes in particular (GLMM: estimate = 4.30, $P = 2.23 \times 10^{-11}$; Fig. 4, *Lower*). There was, however, also a main effect of the type of preceding figure motion: Crossed preceding figure motion led to significantly greater responses (GLMM: estimate = 2.33, $P = 1.22 \times 10^{-14}$) and strikes (GLMM: estimate = 3.81, $P = 1.73 \times 10^{-10}$) during the elementary-motion phase. Almost no mantises made strikes in the uncrossed elementary-motion condition when the preceding figure motion was also uncrossed (Fig. 4*B*). Furthermore, even with crossed elementary motion, strikes in particular were much reduced if the preceding figure motion was uncrossed and only reached an average level comparable to the uncrossed elementary-motion condition with preceding crossed motion (compare crossed condition in Fig. 4 *B*, *Lower* with uncrossed condition in Fig. 4 *A*, *Lower*).

Taken together with the existing literature, our results demonstrate that both figure motion of a prey-like object and stereoscopic disparity indicating that the prey is in range are necessary to elicit mantis strikes. However, our results suggest that these 2 components are governed by distinct systems. The requirement for the correct disparity is demonstrated by the lack of strikes to stimuli containing only uncrossed disparity [Figs. 1–3 and previous studies (29, 30, 32)]. The requirement for figure motion is demonstrated by the lack of strikes to elementary motion within a fixed spatial region with the correct disparity (experiment 1, Fig. 1*E*). However, in experiment 4, we decoupled these and demonstrated that strikes could be elicited by a combination of figure motion with uncrossed disparity followed by elementary motion with the correct disparity. This suggests a stereo-blind system for detecting prey presence, which uses second-order motion cues to detect figure motion, and a stereoscopic system for judging prey distance, which requires only temporal change (30).

Computational Modeling. To formalize how the mantis could detect prey independent of stereo computation, we built a model that detects targets with second-order motion. Some prior models have been proposed for the perception of second-order motion. These are usually based on initial detection via elementary-motion detectors (EMDs) sensitive to first-order motion, followed by subsequent processing to extract second-order motion. The models include full-wave rectification of the EMD output and lateral connections between fine-scale EMDs and large-scale EMDs (9, 13, 15, 39). Our results were reminiscent of earlier results showing that insects can track objects without tracking elementary motion (40). These previous results were modeled as

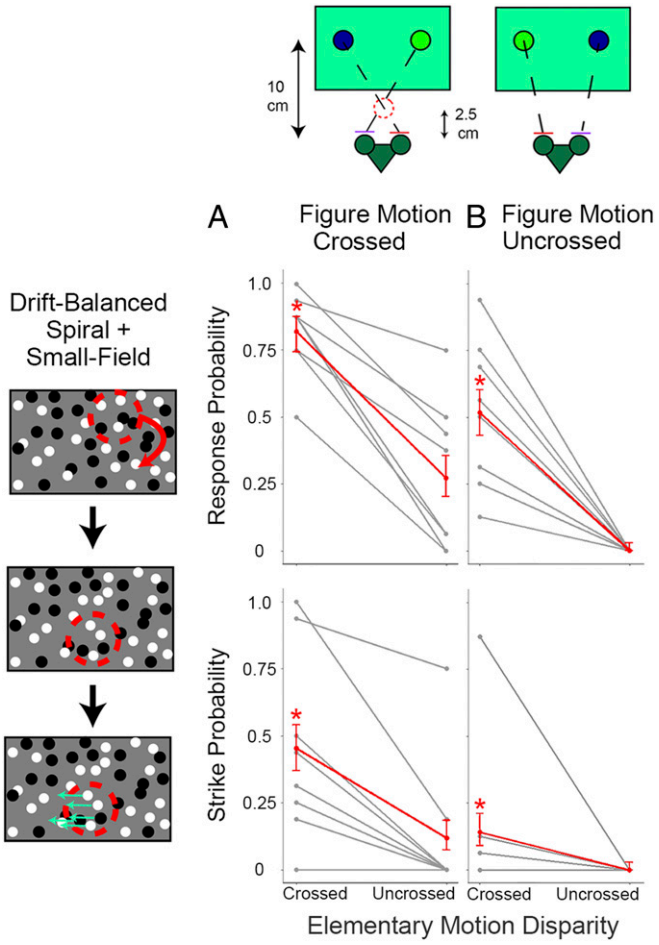

Fig. 4. Experiment 4: Prey-capture responses. The responses are to the elementary-motion phase of the stimulus. The preceding figure motion had either crossed disparity, indicating 2.5 cm (*A*), or uncrossed disparity of the same parallax (*B*). Other details are as in Fig. 1. Stimulus cartoon in *Left* depicts the initial drift-balanced spiral (Fig. 2*A*) with figure motion and the later small-field motion (Fig. 1*E*) with elementary motion. Stimulus cartoon at *Top* depicts the 2 disparity conditions of the figure motion (crossed and uncrossed disparity). $*P < 0.05$.

being driven by position detectors. We therefore implemented a model consisting of 2 layers of detectors where the first layer consisted of position detectors as modeled in ref. 40 (Fig. 5). The second layer consisted of a "second-order motion detector," which comprised a classic EMD (41) but one which took as input the output of the position detectors (Fig. 5 *B–F* and Movies S1–S5, second row). Such a 2-layer model captured our results well, responding selectively to the direction of second-order motion, but not to elementary motion (Fig. 5, Model Response; Movies S1–S5, bottom row).

The first layer of our model consisted of a set of linear, spatiotemporally separable filters (Fig. 5 *A*, *Left*). We can think of these as corresponding roughly to the output of each ommatidium. The spatial filter is Gaussian, with a width designed to reflect the acceptance angle of mantis ommatidia. The temporal filter is a first-order high-pass filter, meaning that the first layer responds only to changes in luminance. The red contour lines in the left column of Fig. 5 *B–F* show the Fourier spectrum of this spatiotemporal filter. It is spatially low pass, but temporally high pass. These contours are superimposed on the Fourier spectra of the stimuli and discussed below.

The outputs of the layer-1 sensors were squared before providing the input to a second layer of EMDs inspired by the model

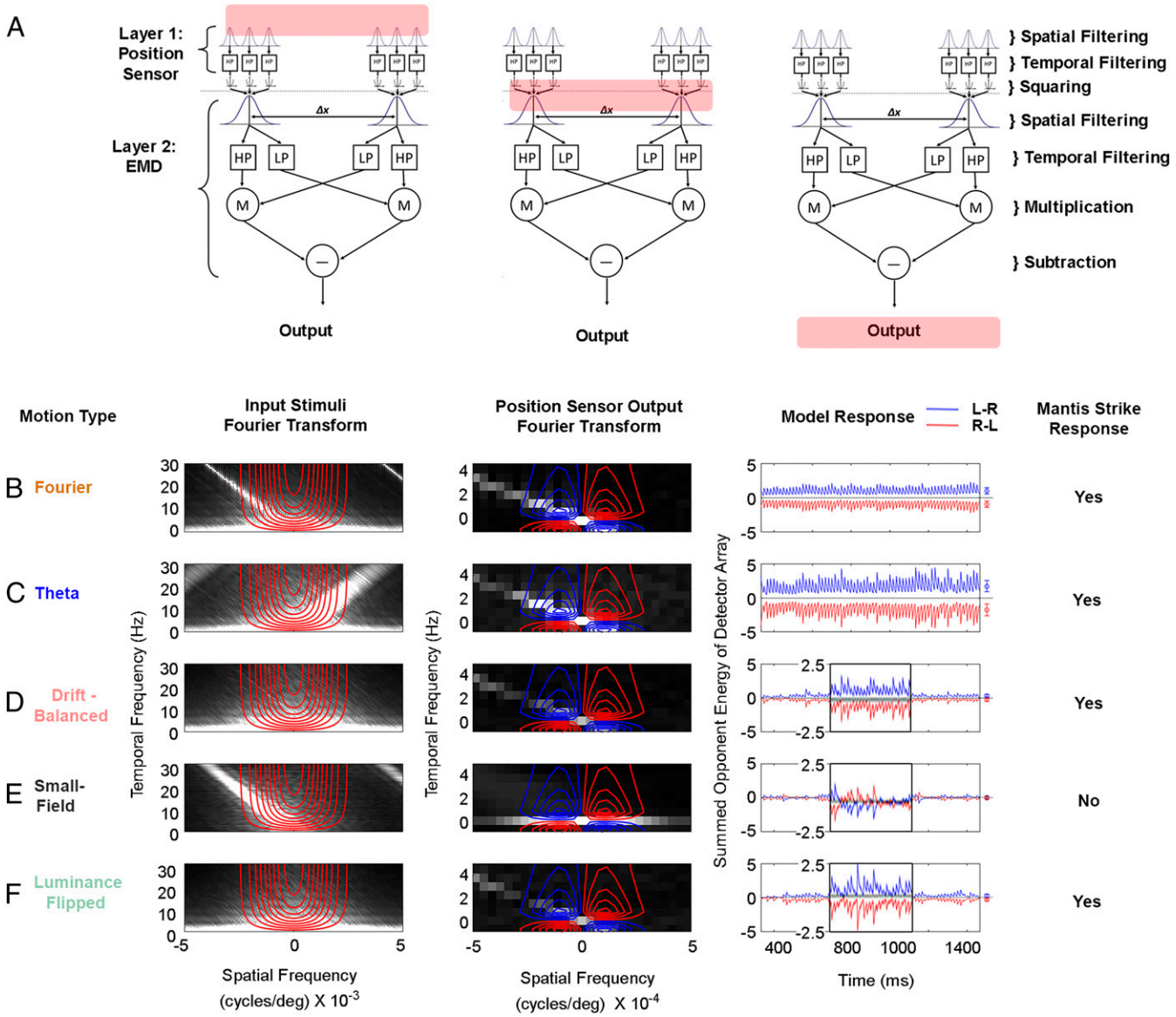

Fig. 5. Computational model of second-order motion detection in the mantis. (*A*) Schematic depiction of the model detecting second-order motion. The model consisted of 1 layer of position detectors feeding into a second layer consisting of EMDs. HP, high-pass filter; LP, low-pass filter; M, multiplication operation. The stimulus and the response of the model at the different stages highlighted by the pink rectangle are shown below. Column 1: Fourier spectra of each of the 5 stimuli input into the model. (*B*) Fourier stimuli. (*C*) Theta stimuli. (*D*) Drift-balanced stimuli. (*E*) Small-field stimuli. (*F*) Luminance-flipped stimuli. All stimuli moved from one end of the screen to the other and were as depicted in Fig. 1, except for the luminance-flipped stimulus, which here moved horizontally across the screen rather than with a spiral motion. We only plot these spectra for left (L)–right (R) motion movies (right–left would appear as an approximate mirror image along the vertical axis). Red contours depict the receptive fields of the position detectors in the first layer of our model; these are drawn at 10% intervals of the maximum response from 90 to 10%. Column 2: Fourier spectra of the output of the first layer of our model with each of the 5 input stimuli. Red and blue contours depict the Fourier response of the EMD in the second layer of the model, calculated as opponent energy, as in figure 2D of ref. 42. These are drawn at 90%, 70%, 50%, 30%, and 10% of the maximum response. Blue contours denote sensitivity to rightward motion and red to leftward. Column 3: Directional output of the second and final layer in the model which consisted of EMDs. Blue lines depict response to stimuli moving left to right, and red lines to stimuli moving right to left. *D–F*, *Insets* show an expanded view. Adjacent box plots represent the mean and SD of the responses—note that the error bars only overlap with 0 for the small-field motion condition. Column 4: Prey detection and capture responses of mantises in our behavioral experiments to each type of stimulus (as shown in Figs. 1 and 2) correspond well with the motion detection output of the model.

of Hassenstein and Reichardt (41). These again had a stage of spatial filtering, pooling many layer-1 sensors with Gaussian weights. This was followed by separate low-pass and high-pass temporal filtering. The low-pass output of 1 layer-2 subunit was multiplied together with the high-pass output of the adjacent subunit, and the results were subtracted to give a direction-selective sensor. The red and blue contour lines in the middle column of Fig. 5 *B–F* show the sensitivity of the EMD after this opponent stage (42).

The grayscale images in the left column of Fig. 5 *B–F* show the Fourier spectra of the different movie stimuli. The Fourier stimulus (Fig. 5*B*) has a series of diagonal stripes representing the first-order motion of the stimulus. The gradient of the line reflects its speed and the upward slope its rightward direction. (The line

repeats along the temporal frequency [vertical] axis, with a spacing of 60 Hz reflecting the 60-Hz frame rate of our stimuli.) The same lines are visible even more in the small-field stimulus (Fig. 5*E*). In the theta stimulus (Fig. 5*C*), similar stripes are visible, but slant downward, reflecting the opposite direction of the first-order motion of this stimulus. In the drift-balanced (Fig. 5*D*) and luminance-flipped (Fig. 5*F*) stimuli, no directional structure is visible in the Fourier spectrum at all. This reflects the purely second-order motion of these stimuli, which by definition is not visible in the Fourier domain.

The grayscale images in the middle column of Fig. 5 *B–F* show the Fourier spectra of the outputs of the first layer, which form the inputs to the second layer (note the different axis range). With the exception of small-field motion (Fig. 5*E*), these each have clear directional power lines which pass through the blue contour and almost entirely miss the red contours. This is exactly as we would expect, as our model is oriented such that left–right motion should produce negative opponent energy. Small-field motion (Fig. 5*E*) does not produce a directional power line at the middle column. This is because in small-field motion stimuli, although there is motion within the target, the target itself does not move across the screen (Movie S4). The right-most column of Fig. 5 *B–F* shows the summed responses of all rightward-sensitive EMD to stimuli moving right (blue) and left (red). The "spikes" visible in the response reflect the model's transient response to each new frame of the movie sequence. For the stimuli in which a target moves across the screen, the response is directional, with a positive response to rightward motion and a negative response to leftward. For the small-field motion stimulus (Fig. 5*E*), which contains only first-order motion within a stationary target, this directional response is much weaker and fluctuates on either side of zero. It would be largely abolished by a threshold. If a suprathreshold response is required for predatory strikes, this could therefore explain why strikes are not observed for stimuli without figure motion.

The critical feature of the model is that it has 2 layers with specific functions. The first layer detects where in the image things are changing. Here, we have implemented this with a simple high-pass filter plus squaring, but many other approaches would also work, e.g., a first layer consisting of EMDs whose output is rectified (9). The second layer then detects the movement of this changing region across the visual field. It is this layer which imposes the requirement for figure motion. We conclude that a 2-layer system of second-order motion detection is a viable model of the input for mantis prey detection.

Discussion

Our results show that prey detection and capture by mantises requires figure motion of the target. The stereoscopic evaluation of depth, however, does not. Mantises are capable of detecting prey and discriminating depth in a range of stimuli with different combinations of first- and second-order motion. Results from both experiments 1 and 2 where drift-balanced and luminance-flipped stimuli only contained directional cues from second-order motion further demonstrate that second-order figure motion is sufficient for prey detection and stereopsis, even with minimal activation of the EMDs and no directional signal in the Fourier spectrum (Fig. 5). The results from experiments 3 and 4, however, show that figure motion is not necessary for stereopsis—mantises are able to discriminate disparity in stimuli with purely elementary motion within a stationary window. For strikes to be released, however, it is important that this is preceded by figure motion of a prey target across the visual field.

This indicates a stereo-blind prey-detection system that requires figure motion and a disparity sensitive stereo-system that computes the distance to targets which can be defined based on any temporal change (e.g., elementary motion), with strikes requiring both to be activated. In experiment 1, when the target lacked figure motion, the prey-detection system was not activated, and there were no strikes (Fig. 1*E*). In experiment 4, when both the preceding figure motion and the elementary motion crossed disparity, we had the most strikes (Fig. 4 *A*, *Lower*) since both systems were strongly activated. When both motions had uncrossed disparity, the stereo system was not activated and we got no strikes (Fig. 4 *B*, *Lower*). However, when the figure motion had crossed disparity and elementary motion has uncrossed disparity, we still got some strikes, even during the uncrossed elementary motion, presumably because of the initial activation of the stereo system by the crossed disparity of the figure motion (Fig. 4 *A*, *Lower*). Crucially, when the figure motion had uncrossed disparity and the elementary motion had crossed disparity, we still got a similar amount of strikes (Fig. 4 *B*, *Lower*). This suggests that to release a strike, prey must be detected, and also within a certain time window (extending at least 1 s) the stereoscopic localization system must indicate an object within range. Thus, while mantis stereopsis exploits temporal change in either elementary or figure motion, the prey-detection system in mantises requires figure motion. A predatory response requires both these systems to be activated, ensuring that the mantis effectively targets attractive moving prey at the right distance. A similar 2-system account is also suggested by recent work investigating motion in depth in praying mantises (43), where the prey-detection system is sensitive to looming, while the stereo system is not. Our 2-layer model of prey detection produced strong, directional responses to all stimuli with figure motion of a target, including where this motion was purely second order. It produced very weak responses to stimuli with only first-order elementary motion and no figure motion. We can therefore account for the observed properties of mantis prey detection by postulating that inputs from left and right eyes are processed in a way similar to our model. In insects, this could potentially be governed by object-tracking neurons and mechanisms (40, 44–47) that are distinct from the optomotor response mechanisms governed by the EMDs.

Previous studies have suggested some functions for insect sensitivity to second-order motion. Such a sensitivity has been suggested to enable tracking of objects with changing luminance correlations such as flapping wings (8). It has also been suggested that sensitivity to some forms of motion like theta motion arises purely as a result of combined sensitivity to other more common types of motion, such as elementary motion and drift-balanced motion (8). Our results here directly implicate sensitivity to second-order motion in prey detection through the detection of figure motion. Investigations into the mechanisms underlying second-order motion sensitivity in flies have provided us with substantial insights. These include the underlying mechanisms and the neural basis of second-order motion sensitivity (2, 3, 9). Fly turning behavior in response to figure and elementary motion involves a superposition of a short-latency, position-independent response to elementary motion and a large-latency response to figure motion in a central region of the visual field (2). Our results show that mantis prey detection instead relies primarily on figure motion, suggesting that it is the latter position-dependent response that is implicated. This seems appropriate for 2 reasons. Firstly, our stimuli lack wide-field motion and would not have triggered the EMD-dependent optomotor response. Secondly, the prey-capture response appears to rely on the moving prey being in the foveal position and thus would be driven by the figure motion response in the central visual field. Since the fly experiments relied on bar stimuli compared to our smaller disk stimuli, it is, however, not yet clear if our results reflect the same mechanisms as seen in fly experiments or the previously discussed object detection mechanisms.

Kral and Prete (33) identified 10 properties which influence whether mantises classify any given object as prey, including stimulus size and shape, contrast relative to the background, speed, and direction of motion. In launching a strike, stereoscopic

distance is also critical—mantises will strike at virtual prey when binocular disparity is manipulated to indicate that it is present in the catch range and rarely strike at prey where the disparity-defined distance is too great or is undefined (as in our uncrossed condition) (27, 29). Kral and Prete (33) therefore suggested the neat and parsimonious possibility that prey detection and stereoscopic localization are performed essentially in a single step. They postulated that on each side of the brain, a Lobula Giant Motion Detector feeds into a Descending Contralateral Movement Detector, forming a "LGMD–DCMD complex" which acts to detect prey in the corresponding eye (33, 48, 49). These would be tuned to the monocular properties of prey such as size, speed, and also retinal location. The 2 LGMD–DCMD complexes would synapse onto the motor neurons responsible for striking, and strikes would occur when the total input exceeded a threshold. Under normal circumstances, activity in both the left- and right-eye LGMD–DCMD complex would be required to exceed threshold. The tuning of each complex to monocular retinal location would ensure that strikes occurred preferentially to stimuli with the correct binocular disparity, explaining mantis stereoscopic vision. This is an elegant account of mantis stereopsis; so simple, indeed, that Kral and Prete (33) did not consider it stereopsis at all.

Recent neurophysiological evidence (50) has undermined this account, showing that mantis lobula complex—and even the medulla, still earlier in visual processing—already contains binocular information. The present results, suggesting separate systems for prey detection and stereoscopic distance, are also hard to reconcile with the Kral and Prete (33) model. In their unified model, disparity discrimination in the elementary-motion stimulus would require activity in prey-detector neurons. But if elementary motion could activate these neurons, one would expect strikes whether or not crossed elementary motion was preceded by figure motion, and this was not observed (Figs. 2 and 4).

The dependency of mantis prey detection on second-order figure motion rather than first-order motion suggests an ecologically adaptive explanation for second-order motion sensitivity. It would be useful for object-detection systems to be tuned to the movement of the prey itself rather than to features on the surface of the prey. This would, for example, allow the tracking of a ladybug or a butterfly without the potential confusion caused by the movement of dots on the surface of their wings in flight. Second-order motion sensitivity would also allow animals to detect moving prey that are featureless objects that exactly match the luminance of their background (17); such prey would be invisible to first-order motion detectors. It could also counteract the effects of dazzle coloration that relies on high-contrast internal patterns, which interfere with the perception of target speed and direction (51, 52). Our study adds to growing evidence that insect visually guided predation is surprisingly complex, combining several distinct visual processes to enable target detection with maximum flexibility and power.

Methods

Experimental Model and Subject Details. All experiments were conducted on adult female mantises of the species *Sphodromantis lineola*. Mantises were housed individually in semitransparent cages (7 × 7 × 9 cm) in a climate-controlled environment maintained at a temperature of 25 °C. Mantises were fed 1 cricket 3 times a week. During experiments, mantises were not fed, in order to maintain motivation. Experiments were conducted in a within-subject design, so all mantises experienced all experimental conditions.

Method Details.

Preparing and fixing the 3D glasses. Color filters (LEE filters 135 Deep Golden Amber and 797 Purple) were used to deliver anaglyph 3D images. These filters differed from previously used filters (29), but also achieved separate presentation of images to each eye based on spectral content. The transmittance spectra of these filters are provided in ref. 43. Tear-drop-shaped glasses were cut out of the filters with a maximum diameter of 7 cm. Mantises were placed in a tabletop freezer (Argos Value Range catalog no. DD1-05 Tabletop Freezer) for 5–8 min to temporarily immobilize them. They were subsequently pinned down using modeling clay, and the glasses were affixed to the frons of mantises using beeswax applied with a wax melter (Denta Star catalog no. S ST 08). The glasses were fixed so that a different color filter covered each eye. Mantises were then released and allowed to recover overnight before any experiments were conducted.

Visual stimulation and experiments. Mantises were fixed to a stand by means of a small component fitted onto their backs with beeswax. They could hold onto a moveable cardboard disk with their feet and move their head and body, as well as make strikes with their forearms. They were placed so that their eyes were 10 cm away from the screen.

Visual stimulation was provided at a frame rate of 60 Hz on a DELL U2413 LED monitor (1,920 × 1,200 pixels; 51.8 × 32.4 cm). The output of the blue and green channels was digitally adjusted to compensate for the unequal levels of light transmitted through the blue and green filters. The blue channel was thus set at 13% the output of the green channel. The background for all stimuli consisted of blue and green dots against a cyan background. The dots had a diameter of 25 pixels (1.8°) and a density of 55 dots in every 100 × 100 pixel square: 50% of the dots at the maximum luminance ("white" dots) and 50% at the minimum luminance ("black" dots). Through the glasses, each eye would be able to see only blue or green dots as dark and light dots against a "gray" background. The dots were uncorrelated across the 2 eyes, i.e., each eye saw a completely different dot pattern (30).

Prior to all experiments, mantises were tested for motivation by using a dark disk that spiraled in from the periphery to the center. The size and disparity of this disk was chosen to simulate a target of 1-cm diameter, 2.5 cm from the mantis. This is a stimulus that mantises respond to strongly and strike at. Experiments were therefore only carried out if mantises first struck at 2 consecutive presentations of this stimulus. Similarly, the data from an experiment were excluded if the mantis didn't meet the same criterion after the experiment was carried out. Across all experiments, 14 experimental runs of 6 animals out of 133 were excluded.

Experimental stimuli were presented in 2 disparity conditions (Fig. 1*A*). In the first, "crossed" disparity condition, the target regions had positions on the screen such that the lines of sight from each eye crossed at a distance of 2.5 cm from the mantis (7.5 cm from the screen). In the uncrossed disparity condition, the positions of the target regions were reversed, so that they had the same parallax, but with left and right swapped between the 2 eyes. Since the parallax between these regions was greater than the interocular distance for mantises (~0.7 cm), this resulted in the lines of sight not intersecting, and therefore the distance to the mantis was undefined.

Experiment 1. We presented 8 mantises with 4 experimental stimuli in each of the 2 disparities, making for a total of 8 conditions. Each of these conditions was presented to a mantis in interleaved trials with a randomized order in an experimental run. One experimental run had 4 replicates of each condition, and each mantis was tested in 3 experimental runs. This made for a total of 12 replicates per condition for each mantis. One mantis was tested in only 2 experimental runs and thus had only 8 replicates per condition. The 4 stimuli used had different types of motion: Fourier motion, theta motion, drift-balanced motion, and small-field motion.

The Fourier motion stimulus consisted of a target disk with dots like the background pattern (Movie S1, *Upper*). This target disk moved horizontally from one side of the screen to other, starting at three-fourths of the length toward one end of the screen and ending at the other end of the screen—thus covering three-fourths the length of the screen. The target moved with a speed of 82°/s (as measured in the center of the screen), occluding the background as it moved. Thus, the motion of both the target figure and the elementary dots comprising was exactly the same. In half the presentations, the target moved from left to right, and in the other half, the target moved from right to left.

The theta motion stimulus was the same as the Fourier motion stimulus, except that the dots comprising the target disk moved in the opposite direction to the disk at the same speed (Movie S2, *Upper*). In this stimulus, the figure motion was thus opposite to the first-order elementary dot motion.

The drift-balanced stimulus consisted of a notional region that moved as described above. However, no dots moved in this region. The effect was of a moving hole in the background revealing a different dot pattern behind the background (Movie S3, *Upper*). This stimulus thus had no first-order elementary motion, but had second-order figure motion.

For the small-field motion stimulus (Movie S4, *Upper*), the target regions were stationary in front of the mantis with a parallax between the 2 eyes, such that the lines of sight to the regions crossed 2.5 cm in front of the

mantis in the crossed-disparity condition. The dots within each region moved from one edge of the region to the other edge, where they disappeared. As the dots moved, they were replaced at the initial edge by newly generated dots, resulting in a streaming motion of the dots from one end of the region to the other. This stimulus thus had no second-order figure motion, but had first-order elementary motion of the dots.

Experiment 2. In the second experiment, we presented 10 mantises with 3 randomly interleaved stimuli presented in both crossed and uncrossed disparity conditions. Each experimental run consisted of 6 presentations of each of the 3 stimuli in each of the 2 disparity conditions, making for a total of 36 trials per experimental run. Two experimental runs were conducted per animal, making for a total of 12 replicates per animal for every combination of stimulus and disparity condition. In the first 2 stimuli, the background dots were uncorrelated across both eyes, while the last one consisted of correlated dots. The first of the 3 stimuli was a drift-balanced stimulus that spiraled in from the periphery of the screen to the center in front of the mantis. As above, the effect was of a moving hole revealing a different dot pattern behind the background. The motion was a spiral motion, which was the same as that described before (29) and is known to elicit strikes. The second stimulus was a luminance-flipped stimulus consisting of a target region that also moved with this same spiraling motion. As the target regions in each eye moved over the dots in the background, the dots changed their luminance polarity, i.e., black dots became white, and white dots became black. When the region moved on, they reverted to their original polarity. The third stimulus consisted of background and target dots that were correlated across both eyes. The target was a disk with dots on it that moved with the spiraling motion described and obscured the background dots as it moved. The target dots and the disk thus had the same motion, providing both first- and second-order motion cues.

Experiment 3. In the third experiment, we tested whether mantises would strike at and discriminate disparities of targets without figure motion and only elementary motion if these targets had been previously cued by figure motion. The idea was that mantises might potentially use the figure motion to recognize and track an object and then subsequently could use elementary motion to make disparity calculations about the object. We therefore presented 8 mantises with stimuli that consisted of 2 motion phases. In the first, the stimulus consisted of a drift-balanced spiral as described above that vanished when it reached the center of the screen in front of the mantis. This first phase was indicated by an indicator black dot at the bottom of the screen. This dot was hidden from the mantis's view by a small cardboard square, but reflected into the camera's view using a mirror. After a second's pause, the mantis was then presented with the second phase of the stimulus, and the indicator dot vanished. This consisted of a target defined by dots all moving in one direction within the boundary of the target. This target was exactly as in the small-field stimulus described in experiment 1, with the dots streaming within the circular target and vanishing at the edge of the circle, only to be replaced by other dots on the other side. There were 2 figure-motion disparity conditions for the combined stimulus and 2 elementary-motion disparity conditions. The figure-motion conditions consisted of crossed disparities, simulating a distance to the mantis of 2.5 and 5 cm in separate trials. The elementary-motion conditions consisted of crossed and uncrossed disparities both with the same parallax, which simulated a distance from the mantis of 2.5 cm in the crossed condition. Mantises were presented every combination of these 4 conditions in randomly interleaved trials. Each experimental run consisted of 8 replicates of every combination of these conditions. Two experimental runs were conducted for each mantis, making for a total of 16 replicates per condition for each animal.

Experiment 4. In this experiment, we tested whether mantises would strike at and discriminate disparities of targets with only elementary motion if these targets had been previously cued by crossed or uncrossed figure motion. All details were as for experiment 3, except that the figure motion conditions in the first phase consisted of crossed and uncrossed disparities in separate conditions. In the crossed-disparity conditions, the target was simulated to be at 2.5 cm, while the uncrossed condition had the same parallax, but with left and right eyes swapped. This experiment was run with 8 mantises.

Quantification and Statistical Analysis. All responses of the mantises were recorded with a Kinobo USB B3 HD Webcam (Point Set Digital Ltd,.) placed directly under the mantis. The recordings were made so that the screen was not visible in the recording and was thus blind to the experimental condition. These movies were then coded blind to the condition for 3 types of behaviors: tracks, strikes, and tensions. Tracks were sharp movements of the head in response to visual stimuli. Strikes were rapid extensions of the forelegs to capture prey targets perceived to be nearby. Tensions were preparatory movements for a strike, which was eventually unreleased. The number of each of these responses was noted, and the number of strikes and tensions added to obtain the number of prey-capture-related responses. In experiments 3 and 4, the presence of the indicator dot in the movie was used to classify responses to the 1st and second phases of the experiments.

Since the data from the responses were binomial (response or no response), we used a logit link function in GLMMs to analyze the data. With this function, we thus model the log of the odds ratio and fit the estimated parameters for each variable as per the equation:

$$\log(P/(1-P)) = \beta_0 + \beta_1 X_1 + \beta_2 X_2 + \ldots,$$

where P is the probability of a response, β_0 is the parameter estimate for the intercept, and β_i is the parameter estimate for the variable X_i. The estimates of effect size we report for each variable are these estimated parameters. They are thus the change in the log of the odds ratio of the response associated with change in each variable. The generalized model used a maximum-likelihood Laplace approximation to generate the estimates. In all experiments, the response variable was the probability of a prey-capture response ("yes" or "no") and the factors were the animal and the disparity condition. We looked for the main effect of disparity in each motion condition. All data analyses were carried out by using R Studio (RStudio, Inc., Version 1.1.383). Models were built for all experiments with motion condition and disparity as main factors and animal identity as a random factor. Models were used to interpret the results at a significance level of 0.05. In experiment 1, motion condition was coded as a categorical variable, and the effect of each level (Fourier motion, theta motion, and drift-balanced) was compared to a default of the small-field condition. In experiment 2, the motion condition had 3 categories corresponding to the luminance-flipped stimulus, the drift-balanced spiral stimulus, and the correlated disk stimulus, with the first being the default value. In experiment 3, the movies were coded separately for the first 5 s and for the last 3 s, as these time windows corresponded to the figure-motion and elementary-motion phases, respectively. Data from both these were analyzed separately with models as described above. Motion condition for both these analyses was a categorical variable, with 2 categories corresponding to the figure motion in the initial phase indicating target distances of 2.5 and 5 cm. The fixed effect reported in all cases was estimated by using a maximum-likelihood Laplace approximation.

Modeling. The mantis's responses to the various visual stimuli used to obtain our experimental data are well described by the 2-layer model depicted in Fig. 5*A*.

Each of the types of stimuli displayed to the mantis were used as an input to our model. For this, we used a sampling rate of 300 Hz, or 5 times the frame rate of each stimulus, i.e., every frame of the stimulus movie was presented to our model 5 times before moving on to the next frame. Our stimuli for each type of motion were rendered as movies with 88 frames, where each frame was a 2D pixel array with dimensions equal to the monitor screen we used (1,200 × 1,920 pixels). The motion in these stimuli was always along the horizontal axis (1,920 px), and as the simulated bug diameter was only 148 pixels, we cropped each frame to 200 × 1,920 pixels. Therefore, the raw stimuli for each type of motion were 3D pixel arrays with dimensions 200 × 1,920 × 88; however, the sampling rate we used meant that the stimuli that were actually used as the input to our model were 3D pixel arrays with dimensions 200 × 1,920 × 440.

Our model comprised a layer of position sensors feeding into a layer of second-order motion detectors. The first layer of the model was composed of position sensors, which we implemented in a similar way to Bahl et al. (40), whereby each stimulus was passed through low-pass spatial filtering and high-pass temporal filtering. We used a Gaussian spatial filter and set the SD to 10 pixels (or ∼0.72°). This corresponded to the mantis's ommatidial spacing, which ranged between 0.6° and 2.5° depending on the distance of the ommatidia to the fovea (53). We then passed the spatially filtered stimulus through a first-order high-pass Butterworth temporal filter, with a time constant of 20 ms, as used by Bahl et al. (40). The red contour lines in the left column of Fig. 5 *B–F* show the Fourier amplitude spectrum of the resultant spatiotemporal filter. For the purposes of labeling the axes of Fourier spectra in Fig. 5, we approximated each pixel as subtending a constant value of 0.0717°, ignoring changes across the screen plane due to the short viewing distance. We also removed the first 40 frames from the output of the first layer to ensure that any effects of an onset transient (visible in Movies S1–S5) were not included in the Fourier transform depicted in the middle column of Fig. 5.

Finally, we took the squared output of the temporal filter, which now represents the output of the first layer of our model. The output of the first

layer of our model was then used as input to the second layer, which formed our second-order motion detector and was formally equivalent to the EMD model described in ref. 41. This layer again began with a Gaussian spatial filter, this time much coarser, with an SD of 80 pixels, or ∼5.74° (averaged across the screen for an observer at 10-cm distance). The spatially processed stimuli were then each separately passed through low-pass and high-pass temporal filters. We used first-order Butterworth filters again and set the time constants for the low- and high-pass filters to be 200 and 250 ms, respectively.

The EMD comprised 2 pairs of such outputs, called subunits, where one subunit was offset from the other by 148 pixels horizontally (∼10.61° averaged across the screen), equivalent to the diameter of the target. The low-pass output from 1 branch of the EMD was then multiplied by the high-pass output from the other branch, producing 2 multiplication terms. Subtracting one term from the other then gives the sign and magnitude of motion in the stimuli. The red and blue contour lines in the middle column of Fig. 5 *B–F* show the Fourier amplitude response of the EMD, calculated as opponent energy, as in figure 2D of ref. 42. The values used for the subunit separation, spatial filter SD, and the temporal filter time constants were chosen such that the power line in the Fourier amplitude spectrum of the model output would pass through the center of the of the blue contours seen in Fig. 5*B*. These contours indicate the spatial-temporal frequencies that our model is most sensitive to.

Data Availability. Data are available on Figshare at https://doi.org/10.6084/m9.figshare.8944910.v1.

ACKNOWLEDGMENTS. V.N., J.O.K., D.U., and A.S. were funded by a Leverhulme Trust Research Leadership Award RL-2012-019 (to J.C.A.R.). V.N. is also supported by Biotechnology and Biological Sciences Research Council David Phillips Fellowship BB/S009760/1. The stimulus programs are based on previous code written by Dr. Ghaith Tarawneh (Newcastle University).

1. J. W. Aptekar, M. A. Frye, Higher-order figure discrimination in fly and human vision. *Curr. Biol.* **23**, R694–R700 (2013).
2. J. W. Aptekar, P. A. Shoemaker, M. A. Frye, Figure tracking by flies is supported by parallel visual streams. *Curr. Biol.* **22**, 482–487 (2012).
3. Y.-J. Lee, K. Nordström, Higher-order motion sensitivity in fly visual circuits. *Proc. Natl. Acad. Sci. U.S.A.* **109**, 8758–8763 (2012).
4. A. M. Derrington, D. R. Badcock, Separate detectors for simple and complex grating patterns? *Vision Res.* **25**, 1869–1878 (1985).
5. M. Edwards, D. R. Badcock, Global motion perception: No interaction between the first- and second-order motion pathways. *Vision Res.* **35**, 2589–2602 (1995).
6. C. Chubb, G. Sperling, "Second-order motion perception: Space/time separable mechanisms" in *Proceedings: Workshop on Visual Motion* (IEEE, Piscataway, NJ, 1989), pp. 126–138.
7. J. C. Theobald, B. J. Duistermars, D. L. Ringach, M. A. Frye, Flies see second-order motion. *Curr. Biol.* **18**, R464–R465 (2008).
8. J. C. Theobald, P. A. Shoemaker, D. L. Ringach, M. A. Frye, Theta motion processing in fruit flies. *Front. Behav. Neurosci.* **4**, 35 (2010).
9. T. Quenzer, J. M. Zanker, Visual detection of paradoxical motion in flies. *J. Comp. Physiol. A* **169**, 331–340 (1991).
10. E. I. Nitzany, J. D. Victor, The statistics of local motion signals in naturalistic movies. *J. Vis.* **14**, 1–15 (2014).
11. R. O. Dror, D. C. O'Carroll, S. B. Laughlin, Accuracy of velocity estimation by Reichardt correlators. *J. Opt. Soc. Am. A Opt. Image Sci. Vis.* **18**, 241–252 (2001).
12. D. W. Dong, J. J. Atick, Statistics of natural time-varying images. *Netw Comput Neural Syst* **6**, 345–358 (1995).
13. J. M. Zanker, Theta motion: A new psychophysical paradigm indicating two levels of visual motion perception. *Naturwissenschaften* **77**, 243–246 (1990).
14. J. M. Zanker, Theta motion: A paradoxical stimulus to explore higher order motion extraction. *Vision Res.* **33**, 553–569 (1993).
15. J. A. Solomon, G. Sperling, Full-wave and half-wave rectification in second-order motion perception. *Vision Res.* **34**, 2239–2257 (1994).
16. A. T. Smith, N. E. Scott-Samuel, First-order and second-order signals combine to improve perceptual accuracy. *J. Opt. Soc. Am. A Opt. Image Sci. Vis.* **18**, 2267–2272 (2001).
17. D. Umeton, G. Tarawneh, E. Fezza, J. C. A. Read, C. Rowe, Pattern and speed interact to hide moving prey. *Curr. Biol.* **29**, 3109–3113.e3 (2019).
18. R. F. van der Willigen, Owls see in stereo much like humans do. *J. Vis.* **11**, 10 (2011).
19. B. Timney, K. Keil, Local and global stereopsis in the horse. *Vision Res.* **39**, 1861–1867 (1999).
20. M. Ptito, F. Lepore, J.-P. P. Guillemot, Stereopsis in the cat: Behavioral demonstration and underlying mechanisms. *Neuropsychologia* **29**, 443–464 (1991).
21. R. Fox, S. W. Lehmkuhle, R. C. Bush, Stereopsis in the falcon. *Science* **197**, 79–81 (1977).
22. A. J. Parker, Binocular depth perception and the cerebral cortex. *Nat. Rev. Neurosci.* **8**, 379–391 (2007).
23. B. G. Cumming, G. C. DeAngelis, The physiology of stereopsis. *Annu. Rev. Neurosci.* **24**, 203–238 (2001).
24. A. E. Welchman, The human brain in depth: How we see in 3D. *Annu. Rev. Vis. Sci.* **2**, 345–376 (2016).
25. A. J. Parker, Vision in our three-dimensional world. *Philos. Trans. R. Soc. Lond. B Biol. Sci.* **371**, 20150251 (2016).
26. V. Nityananda, J. C. A. Read, Stereopsis in animals: Evolution, function and mechanisms. *J. Exp. Biol.* **220**, 2502–2512 (2017).
27. S. Rossel, Binocular stereopsis in an insect. *Nature* **302**, 821–822 (1983).
28. S. Rossel, Binocular vision in insects: How mantids solve the correspondence problem. *Proc. Natl. Acad. Sci. U.S.A.* **93**, 13229–13232 (1996).
29. V. Nityananda *et al*., Insect stereopsis demonstrated using a 3D insect cinema. *Sci. Rep.* **6**, 18718 (2016).
30. V. Nityananda *et al*., A novel form of stereo vision in the praying mantis. *Curr. Biol.* **28**, 588–593.e4 (2018).
31. T. S. Collett, Vision: Simple stereopsis. *Curr. Biol.* **6**, 1392–1395 (1996).
32. V. Nityananda, G. Bissianna, G. Tarawneh, J. Read, Small or far away? Size and distance perception in the praying mantis. *Philos. Trans. R. Soc. Lond. B Biol. Sci.* **371**, 20150262 (2016).
33. K. Kral, F. R. Prete, "In the mind of a hunter: The visual world of the praying mantis" in *Complex Worlds from Simpler Nervous Systems*, F. R. Prete, Ed. (MIT Press, Cambridge, MA, 2004), pp. 75–116.
34. B. Julesz, *Foundations of Cyclopean Perception* (MIT Press, Cambridge, MA, 1971).
35. F. R. Prete, R. J. Mahaffey, Appetitive responses to computer-generated visual stimuli by the praying mantis *Sphodromantis lineola* (Burr.). *Vis. Neurosci.* **10**, 669–679 (1993).
36. S. Rossel, Binocular spatial localization in the praying mantis. *J. Exp. Biol.* **120**, 265–281 (1986).
37. C. Chubb, G. Sperling, Drift-balanced random stimuli: A general basis for studying non-Fourier motion perception. *J. Opt. Soc. Am. A* **5**, 1986–2007 (1988).
38. V. Nityananda, J. O'Keeffe, D. Umeton, A. Simmons, J. C. A. Read, Second-order cues to figure motion enable object detection during prey capture by praying mantises: DATA. Figshare. https://doi.org/10.6084/m9.figshare.8944910.v1. Deposited 17 June 2019.
39. J. M. Zanker, N. R. Burns, Interaction of first- and second-order direction in motion-defined motion. *J. Opt. Soc. Am. A Opt. Image Sci. Vis.* **18**, 2321–2330 (2001).
40. A. Bahl, G. Ammer, T. Schilling, A. Borst, Object tracking in motion-blind flies. *Nat. Neurosci.* **16**, 730–738 (2013).
41. B. Hassenstein, W. Reichardt, Systemtheoretische analyse der zeit, reihenfolgen und vorzeichenauswertung bei der bewegungsperzeption des rüsselkäfers chlorophanus. *Z. Naturforsch. B* **11**, 513–524 (1956).
42. G. Tarawneh *et al*., Invisible noise obscures visible signal in insect motion detection. *Sci. Rep.* **7**, 3496 (2017).
43. V. Nityananda, C. Joubier, J. Tan, G. Tarawneh, J. C. A. Read, Motion-in-depth perception and prey capture in the praying mantis *Sphodromantis lineola*. *J. Exp. Biol.* **222**, jeb198614 (2019).
44. M. F. Keleş, M. A. Frye, Object-detecting neurons in *Drosophila*. *Curr. Biol.* **27**, 680–687 (2017).
45. J. R. Dunbier, S. D. Wiederman, P. A. Shoemaker, D. C. O'Carroll, Facilitation of dragonfly target-detecting neurons by slow moving features on continuous paths. *Front. Neural Circuits* **6**, 79 (2012).
46. P. T. Gonzalez-Bellido, S. T. Fabian, K. Nordström, Target detection in insects: Optical, neural and behavioral optimizations. *Curr. Opin. Neurobiol.* **41**, 122–128 (2016).
47. K. Nordström, D. M. Bolzon, D. C. O'Carroll, Spatial facilitation by a high-performance dragonfly target-detecting neuron. *Biol. Lett.* **7**, 588–592 (2011).
48. F. R. Prete, T. McLean, P. J. McMillin, Responses to moving small-field stimuli by the praying mantis, *Sphodromantis lineola* (Burmeister). *Brain Behav. Evol.* **47**, 42–54 (1996).
49. M. D. Gonka, T. J. Laurie, F. R. Prete, Responses of movement-sensitive visual interneurons to prey-like stimuli in the praying mantis *Sphodromantis lineola* (Burmeister). *Brain Behav. Evol.* **54**, 243–262 (2000).
50. R. Rosner, J. von Hadeln, G. Tarawneh, J. C. A. Read, A neuronal correlate of insect stereopsis. *Nat. Commun.* **10**, 2845 (2019).
51. N. E. Scott-Samuel, R. Baddeley, C. E. Palmer, I. C. Cuthill, Dazzle camouflage affects speed perception. *PLoS One* **6**, e20233 (2011).
52. A. E. Hughes, C. Jones, K. Joshi, D. J. Tolhurst, Diverted by dazzle: Perceived movement direction is biased by target pattern orientation. *Proc. Biol. Sci.* **284**, 20170015 (2017).
53. S. Rossel, Regional differences in photoreceptor performance in the eye of the praying mantis. *J. Comp. Physiol. A* **131**, 95–112 (1979).